Strong Valence-Band Offset Bowing of $ZnO_{1-x}S_x$ Enhances *p*-Type Nitrogen Doping of ZnO-like Alloys

Clas Persson*

Department of Materials Science and Engineering, Royal Institute of Technology, SE-100 44 Stockholm, Sweden

Charlotte Platzer-Björkman,† Jonas Malmström, Tobias Törndahl, and Marika Edoff

Ångström Solar Center, Department of Engineering Sciences, Uppsala University, SE-751 21 Uppsala, Sweden

(Received 28 November 2005; published 4 October 2006)

Photoelectron spectroscopy, optical characterization, and density functional calculations of $ZnO_{1-x}S_x$ reveal that the valence-band (VB) offset $E_v(x)$ increases *strongly* for small S content, whereas the conduction-band edge $E_c(x)$ increases only *weakly*. This is explained as the formation of local ZnS-like bonds in the ZnO host, which mainly affects the VB edge and thereby narrows the energy gap: $E_g(x = 0.28) \approx E_g(\mathrm{ZnO}) - 0.6$ eV. The low-energy absorption tail is a direct $\Gamma_v \rightarrow \Gamma_c$ transition from ZnS-like VB. The VB bowing can be utilized to enhance *p*-type N_O doping with lower formation energy ΔH_f and shallower acceptor state in the ZnO-like alloys.

DOI: 10.1103/PhysRevLett.97.146403 PACS numbers: 71.20.Nr, 61.72.Vv, 78.20.−e, 85.60.Bt

ZnO is utilized in a broad range of semiconductor technologies, and achieving reliable *p*-type bulk ZnO is currently in focus [1,2]. Isovalent anion alloying $ZnO_{1-x}Y_x$ (Y = S, Se, and Te) can improve the ZnO device performances. For instance, Pt contacts on S treated *n*-type ZnO results in Schottky behavior [3] in contrast to the Ohmic interface of untreated Pt/ZnO. In photovoltaics, a ZnO/ZnS(O, OH)/Cu(In, Ga)Se_2 solar cell with ~18% conversion efficiency has been fabricated using chemical bath deposition of the ZnS(O,OH) layer [4] and ~16% using atomic layer deposition (ALD) of $ZnO_{1-x}S_x$ [5]. Pulsed laser-deposited S doped ZnO films by Yoo *et al.* [6] show weak band-gap narrowing [$\Delta E_g = E_g(x) - E_g(\mathrm{ZnO}) \approx 0.12$ eV for $x = 0.14$], obtained from an $\alpha(\hbar\omega) \propto \sqrt{\hbar\omega - E_g}$ fit of the optical absorption, but the spectra exhibit striking low-energy absorption tails. Meyer *et al.* [7] found much larger gap bowing ($\Delta E_g \approx 0.6$ eV for $x = 0.45$) in their radio-frequency sputtered $ZnO_{1-x}S_x$. Gap bowing in $ZnTe_{1-x}(S, Se)_x$ [8] and $Ga(As, P)_{1-x}N_x$ [9,10] have been discussed in terms of localized impurity states in resonance with the host conduction-band (CB) states, producing in-gap defect states. However, the performance of optoelectronic devices depends not only on the band gap, but outermost on the valence-band (VB) offset E_v, the CB edge E_c, as well as the capability to *n*- and *p*-type dope.

In this Letter we report that the $ZnO_{1-x}S_x$ alloy exhibits a very *strong VB-offset bowing* a function of S content. The ultraviolet photoelectron spectroscopy (UPS), optical spectophotometry, ellipsometry, and density functional (DF) calculation reveal (Fig. 1) that the VB offset $E_v(x)$ increases *strongly* whereas the CB edge $E_c(x)$ increases only *weakly* for small S incorporation (i.e., $x < 0.3$). The different behaviors of $E_v(x)$ and $E_c(x)$ yield the strong alloy band-gap bowing, without creating localized CB states below E_c(ZnO). Moreover, the optical characterization depicts a puzzling band-edge absorption of $ZnO_{1-x}S_x$ with an $\alpha(\hbar\omega) \propto (\hbar\omega - E_g)^2$-like behavior on the low-energy side, which could indicate either indirect transitions, off stoichiometry, or the presence of grain-boundary defects. However, the calculated absorption coefficient evinces that this anomalous absorption is indeed direct $\Gamma_v \rightarrow \Gamma_c$ transitions in a defect-free crystalline $ZnO_{1-x}S_x$ structure. We explain both the strong VB-offset bowing and the absorption tail as a consequence of local ZnS-like bonds in the ZnO-like host material. Furthermore, we demonstrate that the ZnS-like VB maximum (VBM) for small S ($0.02 < x < 0.20$) can be utilized for achieving

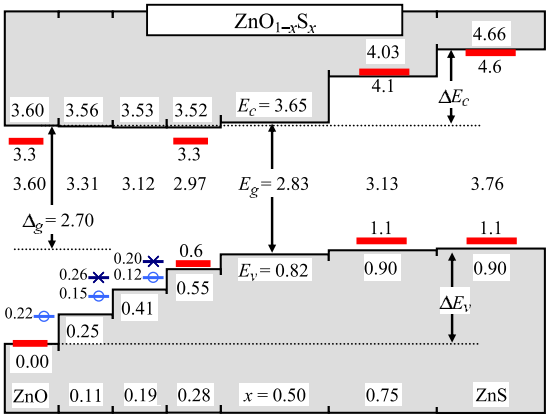

FIG. 1 (color online). Calculated $T = 0$ K VB offset $E_v(x)$, CB offset $E_c(x)$, and band-gap energy $E_g(x)$. Energies are in units of eV, referenced to $E_v(\mathrm{ZnO}) = 0$ eV, and with an estimated error bar of ±0.05 eV. Thick (red) lines show $T = 300$ K results from UPS and optical characterization with ±0.1 eV error bar. (Blue) marks depict calculated ionization energies $E_A = \varepsilon(0/-)$ of N_O acceptors, where × (○) represents N_O with a (with no) neighboring Zn–S bond. The strong VB-offset bowing renders thus shallow ZnO-like N_O acceptors. Measured ZnO:N ionization energy (Ref. [11]) is $E_A \sim 0.21 \pm 0.05$ eV.

stronger p-type character in N doped ZnO-like materials, due to lower N_O acceptor transition energy $\varepsilon(0/-)$, as well as due to lower formation energy $\Delta H_f(N_O)$. This finding is generic for similar alloys involving first row elements (e.g., B, C, N, and O) with short cation-anion bonds.

The $ZnO_{1-x}S_x$ thin films (50–70 nm) are deposited by ALD at 120 °C on glass using $Zn(C_2H_5)_2$, H_2O, and H_2S precursors; see Ref. [5] for details. The S and Zn content in the films are obtained from x-ray fluorescence measurements calibrated by Rutherford backscattering measurements. X-ray diffractograms (XRD) show single phase wurtzite (wz)-like structure for $x = 0$, 0.10, 0.28, 0.84, and 0.97, whereas the $x = 0.48$ film has a weak crystalline structure on top of an amorphous background. The $x = 0.71$ film is completely amorphous; see also Refs. [5,12]. The lattice parameters of the crystalline films follow closely the Vegard's law. The VB offset of the $ZnO_{1-x}S_x$ films is acquired using the He I (21.2 eV) and He II (40.8 eV) lines in UPS [Fig. 2(a)]. Coupling of the ALD reactor to the UPS and x-ray photoelectron spectroscopy chamber allows for determination of the as-deposited, non-air-exposed surface state of the samples. This is very important since the penetration depth in UPS is only a few nm and contamination, or the commonly used surface sputter cleaning, would severely alter the surface. From the secondary electron cutoff in photoemission [PE_{cutoff} in Fig. 2(a)], the work functions ϕ_s of the surfaces were obtained. The photoemission threshold $E_T = \phi_s + E_F - E_v$ (where E_F is the Fermi level) yields the position of VBM relative to vacuum. The VB edge was determined from the He I spectra only since overlap with signals from the He II satellite line at 48.4 eV is expected in the He II spectra. Measured UPS E_T are 8.1 eV (ZnO), 7.5 eV ($x = 0.3$), 7.0 eV ($x = 0.7$), and 7.0 eV (ZnS), marked in Fig. 1. These threshold energies demonstrate that VB offset *increases strongly* for small S incorporations.

The DF calculations are based on the local density approximation (LDA), improved by an on site Coulomb interaction correction within the LDA+U^{SIC} approach [13]. This approach describes the Zn 3d–O 2p hybridization in ZnO better compared to LDA [14]. ZnO and ZnS are calculated with a wz C_{6v}^4 structure. The $ZnO_{1-x}S_x$ alloy is modeled by 72 atom $3 \times 3 \times 2$ wz-like supercells $Zn_{36}O_{36-n}S_n$ with $n = 4$, 7, 10, 18, and 27, representing $x = 0.11$, 0.19, 0.28, 0.50, and 0.75, and with S distributed as uniformly as possible. The correction of the DF/LDA band gap is estimated with a quasiparticle method by Bechstedt and Del Sole [15]. The VB offset is determined from the local VBM of the atomic-resolved density of states (DOS) of various $ZnO_{1-x}S_x/ZnO_{1-y}S_y$ systems; this method has been explored for studying hole barriers of Cu(In, Ga)Se_2 grain boundaries [16]. We use a 288 atom $3 \times 12 \times 2$ supercell slab geometry, oriented in the non-polar $(10\bar{1}0)$ direction to avoid that surface dipoles affect the VB offset. The LDA+U^{SIC} approach improves the LDA band gap, which thereby avoids destructive charge transfers from the VBM of the S-rich side of the slab (with energetically high E_v and E_c) to the CB minimum of the O-rich side (with lower E_v and E_c). We cannot exclude zinc-blende (zb)-like regions in the S-rich ALD samples, but our calculations show that zb-ZnS and wz-ZnS have similar gaps [E_g(wz-ZnS) − E_g(zb-ZnS) = 0.09 eV], and small VB offset [ΔE_v(wz-ZnS/zb-ZnS) < 0.05 eV]; we find similar values for the zb- and wz-ZnO phases.

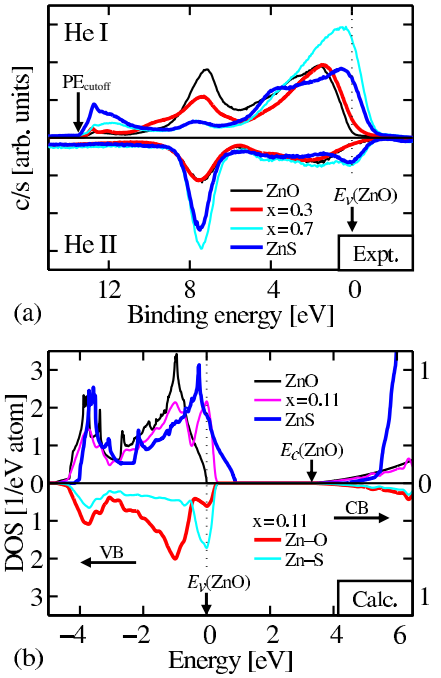

FIG. 2 (color online). (a) UPS energy distribution curves (c/s) referenced to E_v(ZnO) = 0 eV: He I (21.2 eV; upper panel) and He II (40.8 eV; lower panel). Work function ϕ_s is determined from the PE_{cutoff} and VBM is obtained from the leading edge in the He I spectra. (b) Calculated total DOS (upper panel) and atomic-resolved DOS for a Zn–S and Zn–O dimer in $ZnO_{0.89}S_{0.11}$ (lower panel), demonstrating the ZnS-likeVBM.

Consistent with UPS, the DF/LDA+U^{SIC} calculations reveal [Fig. 2(b)] that the VB offset increases *strongly* for small S incorporations. The calculated bond length δ(Zn–anion) is 1.98 Å in ZnO and 2.34 Å in ZnS. We find from geometry optimizations of the supercells that crystallized $ZnO_{1-x}S_x$ preserves *all* these Zn−anion bond lengths [with δ(Zn–O) = 2.02 ± 0.05 Å and δ(Zn–S) = 2.30 ± 0.05 Å] *for all compositions* x. Thus, the bonds are ZnO- or ZnS-like also in the alloy. The upper panel of Fig. 2(b) shows that the DOS of $ZnO_{0.89}S_{0.11}$ follows the ZnO DOS from about −4.5 to −0.5 eV. In the region −0.5 to 0.2 eV the DOS is ZnS-like, whereas the CB is ZnO-like (e.g., the ZnS CB peak at ∼5 eV is not present in $ZnO_{0.89}S_{0.11}$). The local Zn–S bonds in ZnO are reflected in the atom-resolved DOS of $ZnO_{0.89}S_{0.11}$ [Fig. 2(b), lower panel]. Here we compare the DOS for a local Zn–O dimer in $ZnO_{0.89}S_{0.11}$ having no neighboring S atom [thick (red) line in the figure] with a Zn–S dimer [thin (blue) line]. This demonstrates that the VBM of $ZnO_{0.89}S_{0.11}$ consists mainly

of Zn and S. Furthermore, the shorter Zn–O bonds create a strong ZnO-like VB DOS peak ~1.0 eV below the ZnS-like peak. This is similar to GaAs:N where the short Ga–N bond creates a deep VB state ~2 eV below the VBM [17]. Importantly, the CB DOSs of both Zn–S and Zn–O dimers in $ZnO_{0.89}S_{0.11}$ are very similar to CB DOS of ZnO, and thus only the VB is affected by small S incorporation.

Figures. 1 and 2 explain how the ZnS-like bonds in $ZnO_{0.89}S_{0.11}$ strongly raise the VBM for small S content and, at the same time, have no affect on the CB. ZnS has its VBM ~1.0 eV above that of ZnO. Therefore, a hypothetic ZnS cluster with a perfect ZnS-like environment embedded in an otherwise perfect ZnO-host material would form a ZnS-like VB "defect state" at $E_v(\mathrm{ZnO}) + 1.0$ eV, and thus create a band gap of $\Delta_g = 2.70$ eV (Fig. 1). However, in contrast to this hypothetic ZnS cluster, the present adjusted Zn–S dimers are hybridized with the ZnO-host states, and do thus not form localized states, but instead broaden the VB dispersion yielding $E_v(0.11) = E_v(\mathrm{ZnO}) + 0.25$ eV. The local Zn–S bonds in $ZnO_{0.89}S_{0.11}$ will not affect the CB minimum because the lowest ZnS CB states are ~1.0 eV *above* those of ZnO.

The energy gaps of the ALD $ZnO_{1-x}S_x$ films are determined from combined optical spectrophotometry and ellipsometry measurements [18]. The dielectric function $\varepsilon(\hbar\omega)$, along with film thickness and roughness, is obtained by fitting to all energy dependent measurement data simultanously. The XRD characterization and the optical response show no variation with film thickness (up to 300 nm). The absorption coefficient $\alpha(\hbar\omega) = 2\pi\varepsilon_2\hbar\omega/\mathrm{Re}|\sqrt{\varepsilon(\hbar\omega)}|$ of binary ZnO and ZnS exhibit direct VB $\Gamma_v^5 \rightarrow$ CB Γ_c^1 transitions which are fitted by $\alpha(\hbar\omega) \propto \sqrt{\hbar\omega - E_g}$ to yield room temperature $E_g = 3.31 \pm 0.05$ eV (ZnO) and 3.55 ± 0.05 eV (ZnS), where the strong excitonic binding energy of 60 meV in ZnO has been compensated for. However, for the intermediate crystalline $ZnO_{1-x}S_x$ films ($x = 0.10$, 0.28, and 0.84), and to a certain extent also for the partly amorphous films ($x = 0.48$ and 0.71), we find a puzzling band-edge absorption [Fig. 3(a)] that cannot be parameterized by a normal direct transition expression. This anomalous absorption most likely explains the large variation in reported [6,7,12] gap bowing. One may speculate that the absorption tail arises from indirect transitions or defect structures. However, indirect transitions are unlikely because it implies very large energies: $\Delta E(\Gamma_v^5 \rightarrow M_c^2) = 8.5$ eV in ZnO. The present DF calculation [Fig. 3(b)] reveals that the extended absorption tail is indeed arisen from direct $\Gamma_v \rightarrow \Gamma_c$ transitions, and is thus a property of the *crystalline* and *defect-free* $ZnO_{1-x}S_x$ structure. Therefore, based on the analysis of the VB dispersion (Fig. 2), we propose to parameterize the absorption as $\alpha(\hbar\omega) = A\sqrt{\hbar\omega - E_g(\mathrm{ZnO})} + B\sqrt{\hbar\omega - E_g(\mathrm{ZnO}) + \Delta E_g(x)}$. The first (second) term describes the absorption from the ZnO-host (ZnS-like) VBs. This expression represents better the absorption over a wider energy region [inset in Fig. 3(a)]. The fitted band gaps are $E_g(x) = 2.86 \pm 0.05$ eV ($x = 0.10$), 2.71 ± 0.05 eV ($x = 0.28$), and 3.1 ± 0.05 eV ($x = 0.84$). For the amorphous film, $E_g(0.71) = 3.0 \pm 0.1$ eV is extracted from a so-called Tauc plot [19] [$\alpha(\hbar\omega) \propto (\hbar\omega - E_g)^2$], valid for amorphous materials. For the $x = 0.48$ film, fitting to a combined direct band gap and Tauc expression, to account for both crystalline and amorphous parts, gives reasonable agreement with the measured spectrum and $E_g(0.48) = 2.6 \pm 0.1$ eV.

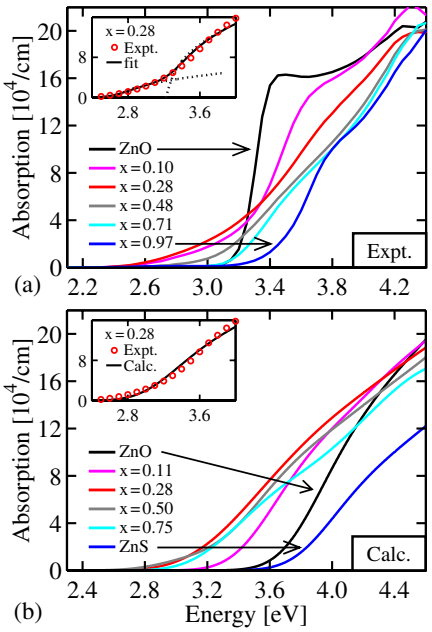

FIG. 3 (color online). (a) Experimental absorption $\alpha(\hbar\omega)$. Inset shows (same units as in main figure) the band-edge absorption of $x = 0.28$ (marks), our proposed parameterization of $\alpha(\hbar\omega)$ with a Lorentzian broadening of $\sigma = 0.15$ eV (solid line), and the two square-root components of the fit (dotted lines). (b) Calculated $T = 0$ K absorption with $\sigma = 0.15$ eV, not including the strong exciton effect in ZnO. The absorption in the inset has been shifted down by 0.2 eV (line) to compare with $T = 300$ K experimental data (marks).

Notice in Figs. 1 and 2 that $ZnO_{1-x}S_x$ exhibits strong band-gap bowing although no localized CB states are energetically below $E_c(\mathrm{ZnO})$; instead the bowing is a consequence of the different behaviors of $E_v(x)$ and $E_c(x)$. Calculations of $Ga(P, As)_{1-x}N_x$ by Bellaiche *et al.* [20] yield also VB bowing. This demonstrates that the theory of impurity states in resonance with host CB states [8–10] needs to be generalized to involve also host VB states in order to fully cover the band-edge physics of alloys. Moreover, the *higher* CB edge in $ZnO_{1-x}S_x$ for $x > 0.5$, *despite a smaller* band gap, explains the Schottky behavior of the sulfur treated Pt/ZnO contact [3], as higher $E_c(x)$ in the S-rich layer and thereby less free carriers there.

Achieving *p*-type bulk ZnO is a major goal for further development of ZnO based technologies. N-doping laser molecular-beam epitaxy with temperature modulation

technique by Tsukazaki *et al.* [1] produces *p*-type ZnO films with $[N] \approx 10^{18} - 2 \times 10^{20}$ cm^{-3}, but highly donor compensated: $N_D/N_A \approx 0.8$. The extraordinary VB offset bowing for small S incorporation can be utilized to enhance *p*-type character in ZnO-like alloys. To demonstrate this, we calculate (see Ref. [21] for details) the N_O transition (ionization) energy $E_A = \varepsilon(0/-) = [E(-) - E(0)] - E_v$ of $ZnO_{1-x}S_x$ [where $E(q)$ is the total energy of the system in charge state q] for a N_O acceptor located either near or far from the ZnS-like bonds in O-rich alloys ($x < 0.20$). Our calculated ionization energy for a single N_O acceptor (i.e., the dilute limit) in ZnO is $E_A(N_O; x = 0) \sim 0.22$ eV, close to measured 0.21 ± 0.05 eV by Wang and Giles [11]. For $ZnO_{1-x}S_x$ and with a ZnS-like neighboring bond (Fig. 1, × marks), the N_O acceptor state is rather deep: $E_A(N_O; x = 0.11) \sim 0.20$ eV and $E_A(N_O; x = 0.19) \sim 0.26$ eV. However, for N_O with a ZnO environment (○ marks) the ionization energy *decreases* from 0.22 eV to $E_A(N_O; x = 0.11) \sim 0.15$ eV and $E_A(N_O; x = 0.19) \sim 0.11$ eV. Furthermore, in *heavily doped* alloys (as for ZnO:N in Ref. [1]) the calculated ionization energies including band filling [21] decreases even further: $E_A(N_O; x = 0) \sim 0.17$ eV, $E_A(N_O; x = 0.11) \sim 0.09$ eV, and $E_A(N_O; x = 0.19) \sim 0.05$ eV. Thus, N_O becomes even shallower at high N concentration.

Hence, S can be introduced to enhance *p*-type doping of ZnO-like alloys. The explanation is that the N_O acceptors with a ZnO environment feel more of the ZnO-like host potential, and becomes thereby shallower with respect to the ZnS-like VBM. That is, since $ZnO_{1-x}S_x$ has a local Zn–S bonding character in the ZnO host, the N_O dopant can be embedded in the ZnO host but with a ZnS-like VBM (Fig. 2). The N_O acceptor with this ZnO-like surrounding can therefore have a different ionization energy than a similar N_O acceptor near a ZnS-like bond.

The neutral N_O acceptor concentration is directly related to the defect formation energy: $\Delta H_f(N_O) = E(0) - E_{host} + (\mu_O - \mu_N)$. The atomic chemical potentials μ_α depend on the growth condition, but the relative change in N_O concentration due to the internal chemical environment is estimated from $\Delta E(N_O) = E(0) - E_{host}$, which is calculated to 1.16 eV for ZnO. From the Boltzmann distribution $[N_O] = N_\alpha \exp(-\Delta H_f(N_O)/k_B T)$, where N_α is the possible impurity site, we estimate the change in N_O concentration at growth temperature $T_g = 450\,^\circ$C. By increasing the S content from $x = 0$ to 0.11 (0.19), $\Delta E(N_O)$ with the ZnO environment is decreased to 1.01 (0.90) eV, $N_\alpha \approx (1\text{–}4x)N_\alpha(x = 0)$ is reduced by 44% (76%), and thereby the N_O concentration is increased by a factor of ~6 (~ 14). The energy $\Delta E(N_O)$ for N close to ZnS bonds is 1.09 (1.02) eV indicating that N_O prefers anion sites with a ZnO environment for $x < 0.20$.

We want to emphasize that the present *p*-type doping model does not involve co- or triple-doping clusters. Instead, the model proposes incorporation of isovalent S-on-O alloy to create high lying VBs. The S concentration should therefore be sufficiently large ($0.02 < x$) to form the ZnS-like VBs to host the N_O holes. However, the S content should not be too large ($x < 0.20$) because that limits the ZnO-like N_O acceptor concentration via N_α. A small S incorporation is expected to have only a minor effect on the minority carriers (the electrons) since the CB is still ZnO-like [Fig. 2(b)].

To conclude: (i) isovalent anion alloy $ZnO_{1-x}S_x$ exhibits a strong VB-offset bowing, caused by local ZnS-like bonds in the ZnO host. A least-squares fit of alloy properties $P_i(x) = P_i(0)(1 - x) + P_i(1)x - b(P_i)(1 - x)x$ yields the VB-offset bowing of $b(E_v) \approx -1.6$ eV. (ii) The CB edge increases weakly for $x < 0.5$ and strongly for $0.5 < x$, thereby yielding $b(E_c) \approx 2.0$ eV. (iii) The puzzling low-energy absorption tail is $\Gamma_v \rightarrow \Gamma_c$ transitions in defect-free crystalline structures. (iv) The improved parameterization of $\alpha(\hbar\omega)$ yields a band-gap bowing of $b(E_g) \approx 3.6$ eV. (v) The strong VB-offset bowing can be utilized to enhance *p*-type doping of ZnO-like alloys ($0.02 < x < 0.20$).

This work is supported by the Swedish Research Council (VR) and the Swedish Energy Agency.

*Electronic address: Clas.Persson@kth.se
†Electronic address: Charlotte.Platzer@angstrom.uu.se

[1] A. Tsukazaki *et al.*, Nat. Mater. **4**, 42 (2005).
[2] F.-X. Xiu *et al.*, Appl. Phys. Lett. **87**, 152101 (2005).
[3] S.-H. Kim *et al.*, Appl. Phys. Lett. **86**, 022101 (2005).
[4] T. Nakada and M. Mizutani, Jpn. J. Appl. Phys. **41**, L165 (2002).
[5] C. Platzer-Björkman *et al.*, J. Appl. Phys. **100**, 044506 (2006).
[6] Y.-Z. Yoo *et al.*, Appl. Phys. Lett. **81**, 3798 (2002).
[7] B. K. Meyer *et al.*, Appl. Phys. Lett. **85**, 4929 (2004).
[8] W. Walukiewicz *et al.*, Phys. Rev. Lett. **85**, 1552 (2000).
[9] S.-H. Wei and A. Zunger, Phys. Rev. Lett. **76**, 664 (1996).
[10] J. D. Perkins *et al.*, Phys. Rev. Lett. **82**, 3312 (1999).
[11] L. Wang and N. C. Giles, Appl. Phys. Lett. **84**, 3049 (2004), and references therein.
[12] B. W. Sanders and A. Kitai, Chem. Mater. **4**, 1005 (1992).
[13] G. Kresse and J. Hafner, Phys. Rev. B **47**, 558 (1993), with PAW, $E_{cutoff} = 380$ eV, 36 **k** points in the irreducible Brillouin zone [172 **k** points for $\alpha(\hbar\omega)$], and $a = 3.253 + 0.569x$, $c = 5.213 + 1.047x$, and $u = 0.380 - 0.005x$. The supercells are fully relaxed with respect to total energy and forces. $U_d(Zn) = 6$ eV in LDA+U^{SIC}.
[14] C. L. Dong *et al.*, Phys. Rev. B **70**, 195325 (2004).
[15] F. Bechstedt and R. Del Sole, Phys. Rev. B **38**, 7710 (1988).
[16] C. Persson and A. Zunger, Appl. Phys. Lett. **87**, 211904 (2005).
[17] C. Persson and A. Zunger, Phys. Rev. B **68**, 035212 (2003).
[18] A. B. Djurišić *et al.*, Mater. Sci. Eng., R **38**, 237 (2002).
[19] J. Tauc, Mater. Res. Bull. **5**, 721 (1970).
[20] L. Bellaiche *et al.*, Phys. Rev. B **56**, 10 233 (1997).
[21] C. Persson *et al.*, Phys. Rev. B **72**, 035211 (2005).